Neurochemical Research (2021) 46:1801–1813
https://doi.org/10.1007/s11064-021-03321-1

ORIGINAL PAPER

miR-671-5p Attenuates Neuroinflammation via Suppressing NF-κB Expression in an Acute Ischemic Stroke Model

Ling Deng[1,2] · Yi Guo[3] · Jingdong Liu[1] · Xuan Wang[1] · Sha Chen[1] · Qian Wang[1] · Jianyan Rao[1] · Yuchun Wang[1] · Tianrui Zuo[1] · Qingwen Hu[1] · Xiahong Zhao[1] · Zhi Dong[1]

Received: 6 January 2021 / Revised: 31 March 2021 / Accepted: 2 April 2021 / Published online: 19 April 2021
© The Author(s), under exclusive licence to Springer Science+Business Media, LLC, part of Springer Nature 2021

Abstract

This study was designed to investigate the role of miR-671-5p in in vitro and in vivo models of ischemic stroke (IS). Middle cerebral artery occlusion and reperfusion (MCAO/R) in C57BL/6 mice as well as oxygen–glucose deprivation and reoxygenation (OGD/R) in a mouse hippocampal HT22 neuron line were used as in vivo and in vitro models of IS injury, respectively. miR-671-5p agomir, miR-671-5p antagomir, pcDNA3.1-NF-κB, and negative controls were transfected into cells using riboFECT CP reagent. miR-671-5p agomir, pcDNA3.1-NF-κB, and negative vectors were administered into MCAO/R mice via intracerebroventricular injection. The results showed that miR-671-5p was significantly downregulated and that miR-671-5p agomir alleviated injury and neuroinflammation induced by ischemic reperfusion. A dual-luciferase reporter assay confirmed that NF-κB is a direct target of miR-671-5p. Reverse experiments showed that miR-671-5p agomir reduced neuroinflammation via suppression of NF-κB expression in both in vitro and in vivo models of IS. Our data suggest that miR-671-5p may be a viable therapeutic target for diminishing neuroinflammation in patients with IS.

Keywords Ischemic stroke · MiR-671-5p · NF-κB · Neuroinflammation

Introduction

Ischemic stroke (IS) is the leading cause of disability worldwide [1, 2], with more than two million young adults suffering from IS episodes each year [3]. Cerebral ischemia, caused by a temporary lack of blood supply to the brain, is known to cause irreversible neuronal death in the brain, which can induce progressive dementia and cognitive deterioration [4]. Many neuroprotective therapies have been revealed as promising prospects in both in vivo and in vitro models of IS, however, their effects on patients have been limited [5–7]. There is still an increased need to seek effective intervention targets to improve neuronal recovery after IS.

MicroRNAs (miRNAs) are small, noncoding rRNAs with lengths less than 50 nucleotides. Recent research has reported that some miRNAs play a role in the translation and transcription process by partially pairing with specific sequences in the 3′ untranslated regions of target mRNAs [8, 9]. In recent years, accumulating evidence has demonstrated that miRNAs have neuroprotective roles in IS [10–13]. miR-675-5p, which is located on chromosome 7 in humans and on chromosome 5 in mice, has been demonstrated to participate in the pathogenesis of various diseases. For example, miR-671-5p was shown to function as a tumor suppressor in osteosarcoma [14] and suppress macrophage-mediated inflammation in orbital fat stem cells [15], while it was also reported to have decreased expression during the oncogenic transition of breast cancer [16] and ameliorate the progression of osteoarthritis [17]. Additionally, a previous study reported that miR-671-5p plays an important role in some central nervous system diseases, such as multiple system atrophy and Parkinson's disease [18]. miR-671-5p is highly abundant in the cerebral cortex, hippocampus, cerebellum, and olfactory bulbs of the mammalian brain, and it is bound

✉ Zhi Dong
100798@cqmu.edu.cn

1 College of Pharmacology, The Key Laboratory of Biochemistry and Molecular Pharmacology, Chongqing Medical University, Chongqing 400016, China

2 Library, Southwest Medical University, Luzhou 646000, Sichuan, China

3 Department of Radiology, Chongqing University Central Hospital, Chongqing 400014, China

with the circular RNA Cdr1, which is important for regulating neuronal activity in human and mouse brains [19]. miR-671-5p has been shown to be a target for reducing neuronal toxicity induced by lead poisoning [20]. IS-induced damage occurs in various brain tissue areas, such as the brain hippocampus, cortex and striatum in animals [21, 22], and neurons are highly sensitive to irreversible damage caused by ischemia and hypoxia [23]. However, little is currently known about whether miR-671-5p plays a role or interacts with a specific target in neuronal injury following IS.

Inflammation plays an important role in the pathogenesis of IS, and an explosive release of some proinflammatory cytokines exacerbates neuronal death in ischemic brain regions [4]. Nuclear factor kappa B (NF-κB) is a transcription factor known to be widely associated with neuroinflammatory responses following ischemic reperfusion, which will induce an explosive release of some proinflammatory cytokines, such as interleukin-1 (IL-1β), interleukin-6 (IL-6), tumor necrosis factor-α (TNF-α), and nitric oxide synthase (iNOS), exacerbating neuronal death [5, 24]. This study was designed to investigate whether miR-671-5p affects the activation of neuroinflammation and its underlying molecular mechanisms in IS. Our results showed that a miR-671-5p agomir sufficiently reduced neuroinflammation via the suppression of NF-κB expression in both in vitro and in vivo models of IS, which indicated that miR-671-5p may be a viable therapeutic target for diminishing neuroinflammation in patients with IS.

Material and Methods

Animals and the Middle Cerebral Artery Occlusion and Reperfusion (MCAO/R) Model

In total, 192 male C57BL/6 mice (20–25 g) were housed under standard conditions (25 °C ± 2 °C, 60–70% relative humidity) with access to food and water ad libitum in the Animal Center of Chongqing Medical University (Chongqing, China). The Chongqing Medical Animal Experiment Center supervised all studies, which were approved by the Ethics Committee of the Animal Laboratory of Chongqing Medical University (License Number: SYXK YU 2010-001). Animal suffering was minimized whenever possible.

The mouse model of IS was developed using the MCAO method based on previously published studies [25]. Briefly, animals were anesthetized using pentobarbital sodium (40 mg/kg; Sunlidabio, Nanjing, China) by intraperitoneal injection and placed in a supine position. Then, the right common carotid artery (CCA), internal carotid artery (ICA), and external carotid artery (ECA) were exposed and dissected away from adjacent nerves. A silicone nylon suture (0.21 mm in diameter; Fengteng Biology, Xi'an, China) was inserted through the CCA into the ICA so that it blocked the middle cerebral artery. This blockage was removed after 60 min (min). The wound was disinfected and sutured. In sham-operated animals, all surgical procedures were identical to the MCAO model, except the silicone nylon sutures were not inserted.

Animal Treatment Groups

For studies of miR-671-5p expression, mice were randomly assigned to five groups: (1) Sham, (2) MCAO/R 0 h, (3) MCAO/R 8 h, (4) MCAO/R 16 h, and (5) MCAO/R 24 h. For studies regarding the mechanistic role of miR-671-5p in MCAO/R mice, the mice were grouped as follows: (1) Sham, (2) MCAO/R, (3) MCAO/R + miR-671-5p agomir, (4) MCAO/R + agomir-negative control (NC), (5) MCAO/R + miR-671-5p agomir + pcDNA3.1-NF-κB, and (6) MCAO/R + pcDNA3.1-NF-κB. The volume of reagent administration to the mice was as follows: 2 μL of miR-671-5p agomir (20 μM; Sagon Biotech, Shanghai, China), 2 μL agomir NC, 2 μL pcDNA3.1-NF-κB (1 ug/μL; GenePharma, Shanghai, China) or 2 μL pcDNA3.1-NC via a right intracerebroventricular injection at 72 h (h) and 24 h before ischemia. Mice in the sham and MCAO groups were administered ddH_2O. Mice hippocampal samples were collected for analysis at MCAO/R after 24 h.

Right intracerebroventricular injection protocol: Mice were anesthetized with pentobarbital sodium (40 mg/kg), fixed, and placed in a prone position on the stereotaxic apparatus (San Diego, USA). The injection site was estimated roughly by 1 mm to the right of the midline of the mouse, using a line drawn through the anterior base of the ears as a guide [26], then a 8–10 mm sagittal incision was made on the scalp of each mouse to expose the bregma. A tiny parietal hole (1.0 mm lateral and 0.5 mm posterior of bregma) was created on the skull perpendicularly by a 1-mm diameter trephine bur, next, a mini-pump syringe (RWD, Ningbo, China) was inserted perpendicularly through the tiny hole into the brain to a depth of 3.0 mm [27]. The mini-pump syringe was inserted into the lateral ventricle when a minute amount of transparent cerebrospinal fluid could be extracted with the empty mini-pump syringe. Finally, the plasmid was injected into the lateral ventricle by the mini-pump syringe at a rate of 0.2 μL/min.

Cell Culture and Oxygen–Glucose Deprivation and Reoxygenation (OGD/R) Treatment

Mice hippocampal HT22 neurons (Zhongqiao Xinzhou Biotech, Shanghai, China) were cultured in a 5% CO_2 incubator in high-glucose Dulbecco's Modified Eagle medium (Saimike, Chongqing, China) with 10% fetal calf

serum (Hyclone, Logan, Utah, USA) and 1% penicillin/streptomycin.

OGD/R treatment: Briefly, normal HT22 cells were transferred to glucose-free DMEM (Gibco, Waltham, MA, USA) for 2 h under hypoxic conditions (1.0% O_2, 93.5% N_2, 5.0% CO_2) at 37 °C. Then, OGD-treated cells were cultured under normal culture media for 24 h to simulate reperfusion. For studies of miR-671-5p expression in OGD/R HT22 cells, we assigned groups as follows: (1) Control, (2) OGD/R 0 h, (3) OGD/R 8 h, (4) OGD/R 16 h, and (5) OGD/R 24 h.

siRNA Transfection

In order to study the role of miR-671-5p in the in vitro model, we designed the groups as follows: (1) Control, (2) OGD/R, (3) OGD/R + miR-671-5p agomir, (4) OGD/R + agomir-NC, (5) OGD/R + miR-671-5p antagomir, and (6) OGD/R + antagomir-NC. In order to study the mechanism underlying the protective role of miR-671-5p, we designed the groups as follows: (1) Control, (2) OGD/R, (3) OGD/R + miR-671-5p agomir, (4) OGD/R + miR-671-5p agomir + pcDNA3.1-NF-κB, and (5) OGD/R + pcDNA3.1-NF-κB. miR-671-5p agomir (50 nM), miR-671-5p antagomir (50 nM), pcDNA3.1-NF-κB (1 μg/mL), and vectors were transfected into cells using riboFECT CP reagent (RIBBIO, Guangzhou, China). Following transfection, cells were subjected to OGD/R treatment and cultured in normal media for an additional 24 h.

Cell Viability Assay

A cell proliferation and cytotoxicity assay kit (methylthiazolyldiphenyl-tetrazolium bromide (MTT; Sigma, St. Louis, MO, USA) was used to measure cell viability according to the manufacturer's protocol. HT22 cells were seeded into 96-well plates at a density of 1×10^4 cells. After each treatment, cells from every group were given 20 μL of MTT (5 mg/mL) and 150 μL of dimethyl sulfoxide (DMSO; Sigma, St. Louis, MO, USA). Then, absorbance was measured using a fluorescence plate reader (Thermo Fisher Scientific, Waltham, MA, USA) at 560 nm.

Lactate Dehydrogenase (LDH) Leakage Assay

Extracellular cytotoxicity was detected using the LDH (Servicebio, Wuhan, China) release assay according to the manufacturer's protocol. Briefly, HT22 cells were seeded into 96-well plates at a density of 1×10^4 cells. After each treatment, 60 μL of culture media from every group was mixed with 60 μL of assay solution and incubated at 22–25 °C for 30 min. Absorbance was measured at 490 nm by using a fluorescence plate reader (Thermo Scientific, USA).

Luciferase Activity

TargetScan 7.2 predicted that NF-κB was a target gene of miR-671-5p (http://www.targetscan.org/mmu_72/). Seed region nucleotides (positions 3284–3289 of NF-κB [Aliases: Rela]) were mutated from GCUUCC to GGUACG as the mutant construct. NF-κB-3′UTR wild-type (WT) or NF-κB-3′UTR mutant-type (Mut) with miR-671-5p mimic or miR-671-5p mimic negative control were co-transfected into 293 T cells (Sangon, Shanghai, China) using RNATransMate (Sangon, Shanghai, China) according to the manufacturer's protocol. The transfected cells were harvested 48 h post-transfection, and the luciferase activity was measured using a Promega dual-luciferase system (Luciferase Assay Reagent, Sangon, Shanghai, China).

Immunofluorescence Staining

Paraffin slices of mouse hippocampal tissue were immersed in xylene for 5 min (twice), 100% ethanol for 2 min, 95% ethanol for 1 min, 80% ethanol for 1 min, and 75% ethanol for 1 min. Antigen retrieval was performed by placing the slides in citrate buffer. Then the slices were washed with 2% phosphate buffer saline (PBS) and 0.3% Triton X (Beyotime, Shanghai, China) for 1 h at 22–25 °C. After washing, the slices were incubated at 4 °C for 24 h with the polyclonal NeuN antibody (1:200, Proteintech, Rosemont, USA). Then the slices were washed three times with PBS for 5 min each and incubated for 30 min with FITC-labeled Goat Anti-Rabbit IgG (H + L) (1: 500, Beyotime, Shanghai, China) at 22–25 °C. DAPI (Beyotime, Shanghai, China) was used for nuclear staining. A fluorescence microscope (Nikon, Tokyo, Japan) was used to image cells.

HT22 cells were seeded into 24-well plates at a density of 1×10^4 cells. After each treatment, HT22 cells were fixed using 4% paraformaldehyde for 20 min. Then the HT22 cells were washed with 2% phosphate buffer saline (PBS) and 0.3% Triton X (Beyotime, Shanghai, China) for 1 h at 22–25 °C. After washing, cells were incubated at 4 °C for 24 h with the primary antibody P65 (1:200, Proteintech, Rosemont, USA). Then the slices were washed three times with PBS for 5 min each and incubated for 30 min with Cy3-labeled Goat Anti-Rat IgG (H + L) (1:500, Beyotime, Shanghai, China) at 22–25 °C. DAPI (Beyotime, Shanghai, China) was used for nuclear staining. A fluorescence microscope (Nikon, Tokyo, Japan) was used to image cells. The fluorescence intensity of P65 in HT22 cells was measured with ImageJ (National Institutes of Health, Bethesda, MD, USA) using the following steps: image → color → split channels, image → adjust → threshold, image → adjust → auto threshold, analyze → measure → values.

Quantitative Real-Time Polymerase Chain Reaction (qRT-PCR)

Trizol (Sagon Biotech) was used to extract RNA from hippocampal tissue samples based on the provided protocol. An all-in-one cDNA Synthesis SuperMix (Bimake, Shanghai, China) was used for cDNA synthesis. The miRNA 1st-Strand cDNA Synthesis Kit (tailing reaction; Sagon Biotech, Shanghai, China) was used for miRNA cDNA. qRT-PCR reactions were conducted to measure miR-671-5p and mRNA NF-κB expression using SYBR Green qPCR Master Mix (Bimake, Shanghai, China). The primer sequences was as follows: mmu-miR-671-5p (sense): 5′-TATAGG AAGCCCTGGAGGGG-3′, universal U6 primer (sense): 5′-CTCGCTTCGGCAGCACA-3′, universal PCR primer (antisense): 5′-AACGCTTCACGAATT-3′, NF-κB (sense): 5′-TGCGATTCCGCTATAAATGCG-3′, NF-κB (antisense): 5′-ACAAGTTCATGTGGATGAGGC-3′, β-actin (sense): 5′-GTGCTATGTTGCTCTAGACTTCG-3′, β-actin (antisense): 5′-ATGCCACAGGATTCCATACC-3′. The Bio-Rad CFX Manager 3.1 system (Bio-Rad, Hercules, CA, USA) was used with the following thermocycler settings: 95 °C for 7 min; 39 cycles at 95 °C for 15 s (s), 60 °C for 40 s, and 65 °C for 30 s. The values of gene expression were directly displayed by the Bio-Rad CFX Manager 3.1 system.

Western Blotting

Samples were lysed using RIPA buffer (Dingguo, Beijing, China) based on the provided protocol. The total protein was separated using a PAGE gel fast preparation kit (Epizyme, Shanghai, China) and transferred to polyvinylidene fluoride (PVDF) membranes (Epizyme, Shanghai, China). The membranes were blocked with bovine serum albumin (Thermo Fisher Scientific, Shanghai, China). The membranes were then incubated with antibodies against p65 (1:2000, Proteintech, Rosemont, IL, USA), phospho-NF-κB p65 (Ser536) (1:2000, Beyotime, Shanghai, China), and β-actin (1:4000, Proteintech, Rosemont, IL, USA), followed by incubation with an anti-rabbit secondary. The membranes were finally exposed using ECL FemtoLight Chemiluminescence Kit (Epizyme, Shanghai, China). The immunoreactive protein expression was quantified using Image Lab3.0 software (Bio-Rad, Hercules, CA, USA) as follows: open → choose lanes → analysis → values, p-P65 or P65 value /β-actin value for each group.

Enzyme-Linked Immunosorbent Assay (ELISA)

HT22 cells were seeded into 6-well plates at a density of 3×10^4 cells. The cell culture medium was collected after each treatment, and HT22 cells were dissociated by 100 µL RIPA buffer (Dingguo, Beijing, China) and pooled for the assay. Hippocampus (18–25 mg) was homogenized in RIPA buffer (10 mg hippocampus: 100 µL RIPA) and diluted up to 1 mL with PBS for the assay. Levels of IL-1β, IL-6, TNF-α, and iNOS in the samples were measured using commercial ELISA kits (Beyotime, Shanghai, China) based on the provided protocol.

Neurological Deficits

At 24 h post-MCAO, the neurological functions of each group of mice were assessed by a blinded researcher using a modified version of a previously reported scoring system [28]. The scoring system was as follows: 0 = no apparent deficits; 1 = difficulty with full extension of the contralateral forelimb; 2 = unable to extend the contralateral forelimb; 3 = mild contralateral circling; 4 = severe circling; and 5 = falling to the contralateral side or death.

Infarct Area

At 24 h post-MCAO, brain tissue was collected and sliced into 1.5-mm thick coronal sections. Sections were stained for 10 min with 2% 2,3,5-triphenyltetrazolium chloride (TTC, Sigma, St Louis, MO, USA) at 37 °C. In the stained sections, infarct tissue appeared white, whereas all other tissue appeared red. In order to evaluate infarction severity, ImageJ was used to measure the area of infarction as a proportion of the total area as follows: infarct area (%) = (infarct area – [the ipsilateral hemisphere area – the intact contralateral hemisphere area]) × 100/intact contralateral hemisphere area [29].

Hematoxylin and Eosin (H&E) Staining

At 24 h post-MCAO, a mouse from every group were anesthetized and transcardially perfused with heparinized saline. Then the mouse brain tissues were fixed using 4% paraformaldehyde (Servicebio, Wuhan, China) for 24 h. Brain tissue were paraffin-embedded, sectioned into 4-µm thick coronal sections, and stained with H&E. Three to five brain sections from every mouse were photographed using light microscopy (Nikon, Tokyo, Japan). Since the nucleus of an injured cell shrinks as compared to a normal cell, we were able to differentiate between injured and normal cells. Percentage of injured cells (%) = injured cell counts × 100/total cell counts [30].

Rotarod Test

Mouse motor coordination was evaluated using a rotarod (Ugo Basile, Italy) before and after cerebral ischemia treatment. Briefly, mice were trained on the rotarod cylinder for 3 days prior to MCAO. The speed was accelerated from four revolutions per minute (rpm) to 40 rpm and lasted no

more than 160 s at baseline [31]. At 24 h post-MCAO, mice were placed on the rotarod device with the same acceleration conditions as above. A researcher blinded to group experiments then observed the motor coordination of the mice and recorded the fall latency time, with a maximum time of 160 s. Animals were tested three times per day with 10 min intervals, and the average time for each animal was calculated.

Statistical Analysis

All data were expressed as the mean ± standard error of the mean (SEM). The experiments were repeated three times in vitro. The number of mice in each group is noted in the legend. Data were compared via one-way ANOVA with Student's *t* test using SPSS v21.0 (IBM, Armonk, NY, USA), with $p < 0.05$ as the significance threshold.

Results

miR-671-5p Expression is Reduced in IS In Vitro and In Vivo

Our results revealed that miR-671-5p was downregulated in hippocampal samples at 8 h (65.94% ± 4.70%, $p < 0.05$), 16 h (67.09% ± 6.33%, $p < 0.05$), and 24 h (54.55% ± 7.87%, $p < 0.05$) post-MCAO as compared to sham control (100.00% ± 0.00%) (Fig. 1a). Similarly, it was found that miR-671-5p expression was significantly decreased in HT22 cells at 0 h (56.02% ± 3.27%, $p < 0.05$), 8 h (70.70% ± 9.99%, $p < 0.05$), 16 h (59.14% ± 7.38%, $p < 0.05$), and 24 h (69.88% ± 11.74%, $p < 0.05$) post-OGD/R as compared to untreated cells (100.00% ± 0.00%) (Fig. 1b). These findings suggested that the expression of miR-671-5p is reduced in the IS model without a fluctuation that ANRIL expression reduced first and then increased. Based on these results, 24-h timepoints were selected for further studies.

miR-671-5p Agomir Reduces OGD/R-Induced Injury and Proinflammatory Cytokines in HT22 Cells

miR-671-5p expression was reduced in the OGD/R group (51.60% ± 8.22%, $p < 0.05$) as compared to the untreated cells (100.00% ± 0.00%). miR-671-5p expression, however, was increased in the miR-671-5p agomir group (188.80% ± 13.36%, $p < 0.05$) and reduced in the miR-671-5p antagomir group (28.25% ± 6.01%, $p < 0.05$) as compared to the OGD/R group. Agomir negative vectors (60.36% ± 8.48%) and antagomir negative vectors (51.42% ± 3.55%) had no impact on miR-671-5p expression (Fig. 2a). This result demonstrated that success upregulation or downregulation of miR-671-5p by transfection with miR-671-5p agomir or antagomir siRNA transfection in vitro.

The MTT results showed that HT22 cell viability was reduced after OGD/R (53.45% ± 3.36%, $p < 0.05$) as compared to the untreated control (100.00% ± 0.00%). OGD/R-treated cell viability was increased by the miR-671-5p agomir (76.17% ± 3.10%, $p < 0.05$) and reduced by the miR-671-5p antagomir (39.69% ± 3.81%, $p < 0.05$) (Fig. 2b). The LDH results showed that HT22 cell cytotoxicity was increased after OGD/R (43.72% ± 0.74%, $p < 0.05$) as compared to the untreated control (11.10% ± 0.48%). OGD/R-treated cell cytotoxicity was reduced by the miR-671-5p agomir (25.11% ± 1.30%, $p < 0.05$) and increased by the miR-671-5p antagomir (46.70% ± 1.98%, $p < 0.05$) (Fig. 2c). mRNA expression of *NF-κB* in HT22 cells was increased in the OGD/R group (366.80% ± 37.21%, $p < 0.05$) as compared to the untreated control (100.00% ± 0.00%). The miR-671-5p agomir (260.40% ± 25.14%, $p < 0.05$) reduced the mRNA expression of *NF-κB*, whereas the miR-671-5p antagomir (481.90% ± 42.88%, $p < 0.05$) had the opposite effect as evidenced by qRT-PCR (Fig. 2d). Western blot analysis results showed that p-P65 and P65 protein levels were increased by OGD/R treatment (p-P65, 0.691 ± 0.043, $p < 0.05$; P65, 0.970 ± 0.049, $p < 0.05$), but the miR-671-5p agomir suppressed p-P65 (0.480 ± 0.033, $p < 0.05$) and P65

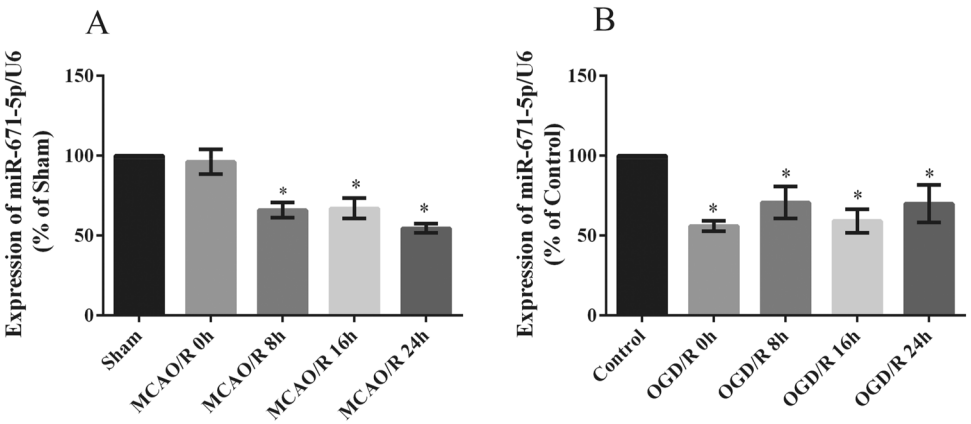

Fig. 1 miR-671-5p expression in the IS model. **a** miR-671-5p levels in murine hippocampal samples (collected at 0, 8, 16, and 24 h post-MCAO) were measured via qRT-PCR ($n = 6$). **b** miR-671-5p expression in HT22 cells was measured at 0, 8, 16, and 24 h post-OGD/R via qRT-PCR (*experiment performed in triplicate*). One-way ANOVA with Student's *t* test, * $p < 0.05$ vs sham or untreated control

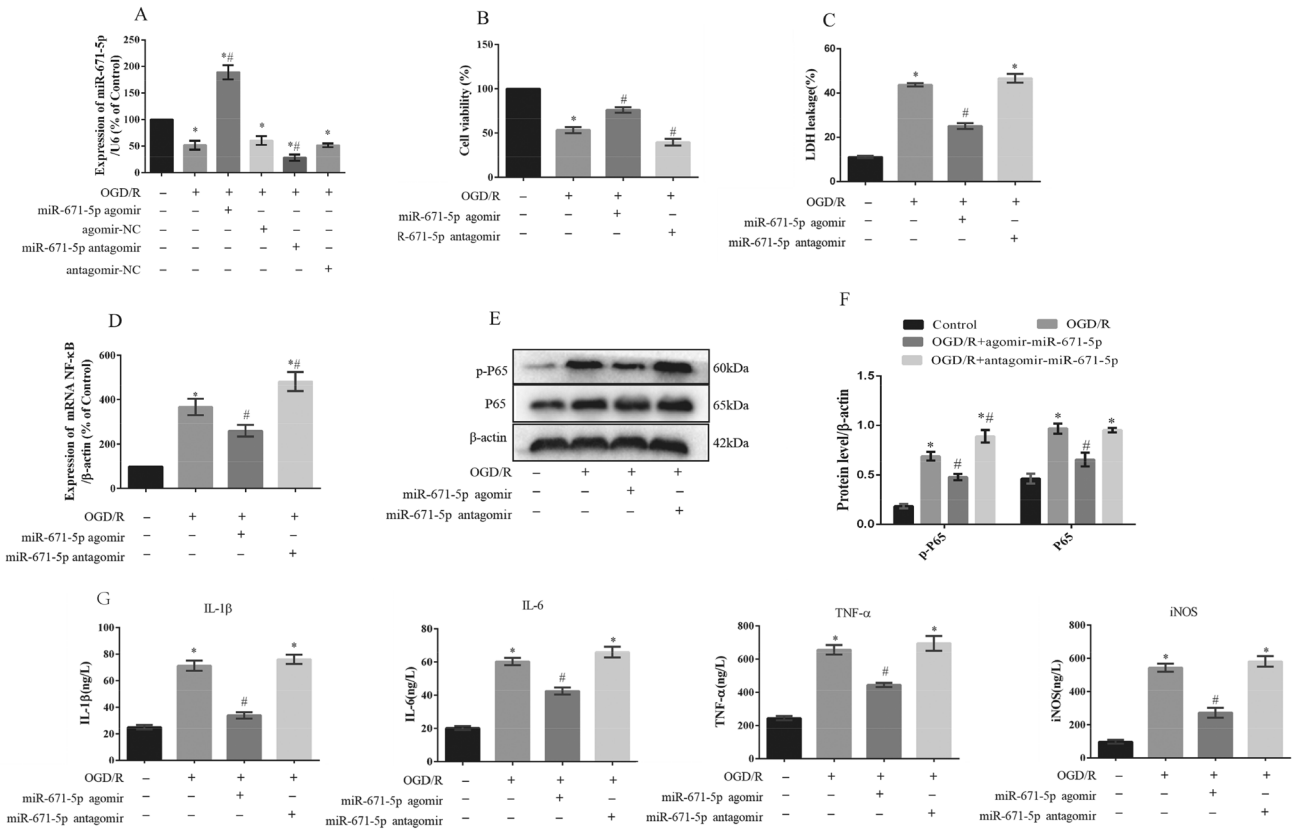

Fig. 2 Impact of miR-671-5p agomir and miR-671-5p antagomir in vitro. **a** Confirmation of successful miR-671-5p upregulation or repression, and no significant effects imposed by the negative control. **b** Cell viability was assessed via a MTT assay. **c** Cell cytotoxicity was assessed via a LDH leakage assay. **d** *NF-κB* mRNA expression was quantified via qRT-PCR. **e**, **f** p-P65 and P65 protein levels were assessed via western blotting. **g** IL-1β, IL-6, TNF-α, and iNOS levels were measured via ELISA. *Experiments were performed in triplicate.* One-way ANOVA with Student's *t* test, $^{*}p < 0.05$ vs control, $^{\#}p < 0.05$ vs OGD/R group

(0.658 ± 0.070, p < 0.05) protein levels (Fig. 2e, f). Proinflammatory factors increased after OGD/R treatment (IL-1β, 71.30 ± 3.82 ng/L, p < 0.05; IL-6, 60.29 ± 2.19 ng/L, p < 0.05; TNF-α, 657.00 ± 28.93 ng/L, p < 0.05; iNOS, 543.9 ± 24.17 ng/L, p < 0.05) as compared with the untreated control (IL-1β, 24.99 ± 1.64 ng/L; IL-6, 20.24 ± 2.00 ng/L; TNF-α, 244.5 ± 12.46 ng/L; iNOS, 97.70 ± 11.37 ng/L), but the miR-671-5p agomir decreased the proinflammatory factors (IL-1β, 33.95 ± 2.38 ng/L, p < 0.05; IL-6, 42.55 ± 2.15 ng/L, p < 0.05; TNF-α, 444.90 ± 12.95 ng/L, p < 0.05; iNOS, 273.10 ± 30.01 ng/L, p < 0.05) as shown by ELISA (Fig. 2g).

NF-κB is a Direct Target of miR-671-5p

TargetScan 7.2 predicted that *NF-κB* was a target gene of miR-671-5p (Fig. 3a). A dual-luciferase reporter show that there was a significant difference between the miR-671-5p agomir group and miR-NC group (p < 0.05) in NF-κB-3′UTR wild-type. However, there was not a significance difference in the NF-κB-3′UTR mutant-type, which indicated that NF-κB is a direct target of miR-671-5p (Fig. 3b).

miR-671-5p Agomir Reduces OGD/R-Induced Neuroinflammation via Suppression of NF-κB Expression

mRNA expression of *NF-κB* in the OGD/R group (159.60% ± 8.08%, p < 0.05) was increased as compared to the untreated control (100.00% ± 0.00%). pcDNA3.1-NF-κB (797.00% ± 71.37%, p < 0.05) enhanced the mRNA expression of *NF-κB*, and pcDNA3.1 negative vectors (173.30% ± 6.39%) had no impact as compared with the OGD/R group. The result demonstrated that pcDNA3.1-NF-κB was able to successfully overexpress the transcript of NF-κB in HT22 cells (Fig. 3c).

We found that cell viability was increased in the miR-671-5p agomir group (79.47% ± 2.58%, p < 0.05) as compared with the OGD/R group (65.37% ± 2.61%), whereas NF-κB overexpression (65.91% ± 2.81%) reversed this effect (Fig. 3d). The LDH results showed that cell

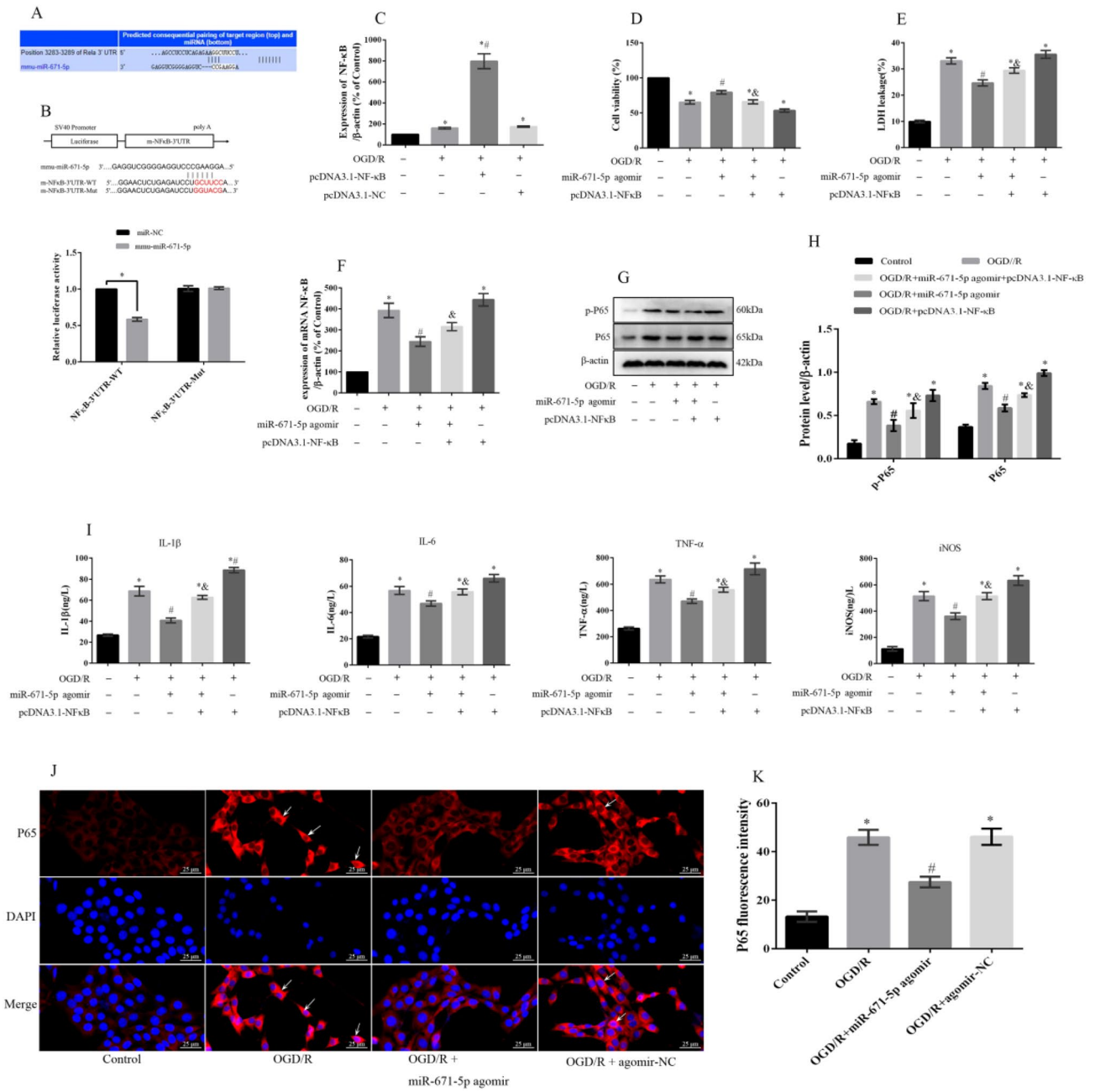

Fig. 3 Impact of miR-671-5P agomir or cotransfection with NF-κB overexpression in vitro. **a** TargetScan 7.2 predicted that NF-κB was a target gene of miR-671-5p. **b** A dual-luciferase reporter assay validated that NF-κB was a direct target of miR-671-5p. **c** Successful overexpression of *NF-κB* mRNA was achieved, and no significant effects imposed by the negative control were assessed via qRT-PCR. **d** Cells viability was assessed via a MTT assay. **e** Cell cytotoxicity was assessed via a LDH leakage assay. **f** *NF-κB* mRNA expression was quantified via qRT-PCR. **g**, **h** p-P65 and P65 protein levels were measured via western blotting. **i** IL-1β, IL-6, TNF-α, and iNOS levels were measured via ELISA. **j**, **k** p65 expression using immunofluorescence staining; white arrow: cells where the fluorescence intensity of p65 is enhanced. *Experiments were performed in triplicate.* One-way ANOVA with Student's *t* test, $^{*}p < 0.05$ vs control, $^{\#}p < 0.05$ vs OGD/R group, $^{\&}p < 0.05$ OGD/R + miR-671-5p + pcDNA3.1-NF-κB vs OGD/R + pcDNA3.1-NF-κB

cytotoxicity was reduced in the miR-671-5p agomir group (24.69% ± 1.15%, $p < 0.05$) as compared with the OGD/R group (33.11% ± 1.15%), whereas NF-κB overexpression (29.45% ± 1.05%) reversed this effect (Fig. 3e). *NF-κB* mRNA expression was significantly reduced in the miR-671-5p agomir group (244.90% ± 22.72%, $p < 0.05$) as compared with the OGD/R group (393.4% ± 34.38%), and this was reversed by overexpression of *NF-κB* (315.80% ± 19.01%) (Fig. 3f). p-P65 and P65 levels were significantly reduced in the miR-671-5p agomir group

(p-P65, 0.384 ± 0.065, $p < 0.05$; P65, 0.586 ± 0.040, $p < 0.05$) as compared with the OGD/R group (p-P65, 0.661 ± 0.030; P65, 0.842 ± 0.035), and this was reversed by overexpression of NF-κB (p-P65, 0.558 ± 0.085; P65, 0.737 ± 0.02) (Fig. 3g, h). The miR-671-5p agomir (IL-1β, 40.82 ± 2.28 ng/L, $p < 0.05$; IL-6, 46.95 ± 2.04 ng/L, $p < 0.05$; TNF-α, 471.50 ± 16.99 ng/L, $p < 0.05$; iNOS, 361.80 ± 25.50 ng/L, $p < 0.05$) also significantly reduced the expression of proinflammatory factors as compared with the OGD/R group (IL-1β, 68.80 ± 4.59 ng/L; IL-6, 56.86 ± 2.97 ng/L; TNF-α, 637.90 ± 26.71 ng/L; iNOS, 514.10 ± 34.60 ng/L). NF-κB overexpression reversed the effect on proinflammatory factors (IL-1β, 62.85 ± 1.84 ng/L; IL-6, 55.86 ± 2.19 ng/L; TNF-α, 558.80 ± 18.75 ng/L; iNOS, 515.10 ± 26.85 ng/L) (Fig. 3i). Immunofluorescence also revealed that the miR-671-5p agomir reduced the OGD/R-induced increases in fluorescence intensity of P65 levels in HT22 cells (Fig. 3j and k).

miR-671-5p Agomir Reduces MCAO/R-Induced Injury

miR-671-5p expression was reduced in the MCAO/R group (69.54% ± 4.89%, $p < 0.05$) as compared with sham group (100.00% ± 0.00%), increased in the miR-671-5p agomir group (193.00% ± 7.21%, $p < 0.05$) as compared with the MCAO/R group, and there were no significant effects caused by the agomir negative controls (61.41% ± 7.94%) (Fig. 4a). These results demonstrated that miR-671-5p expression was successfully upregulated by the miR-671-5p agomir in vivo.

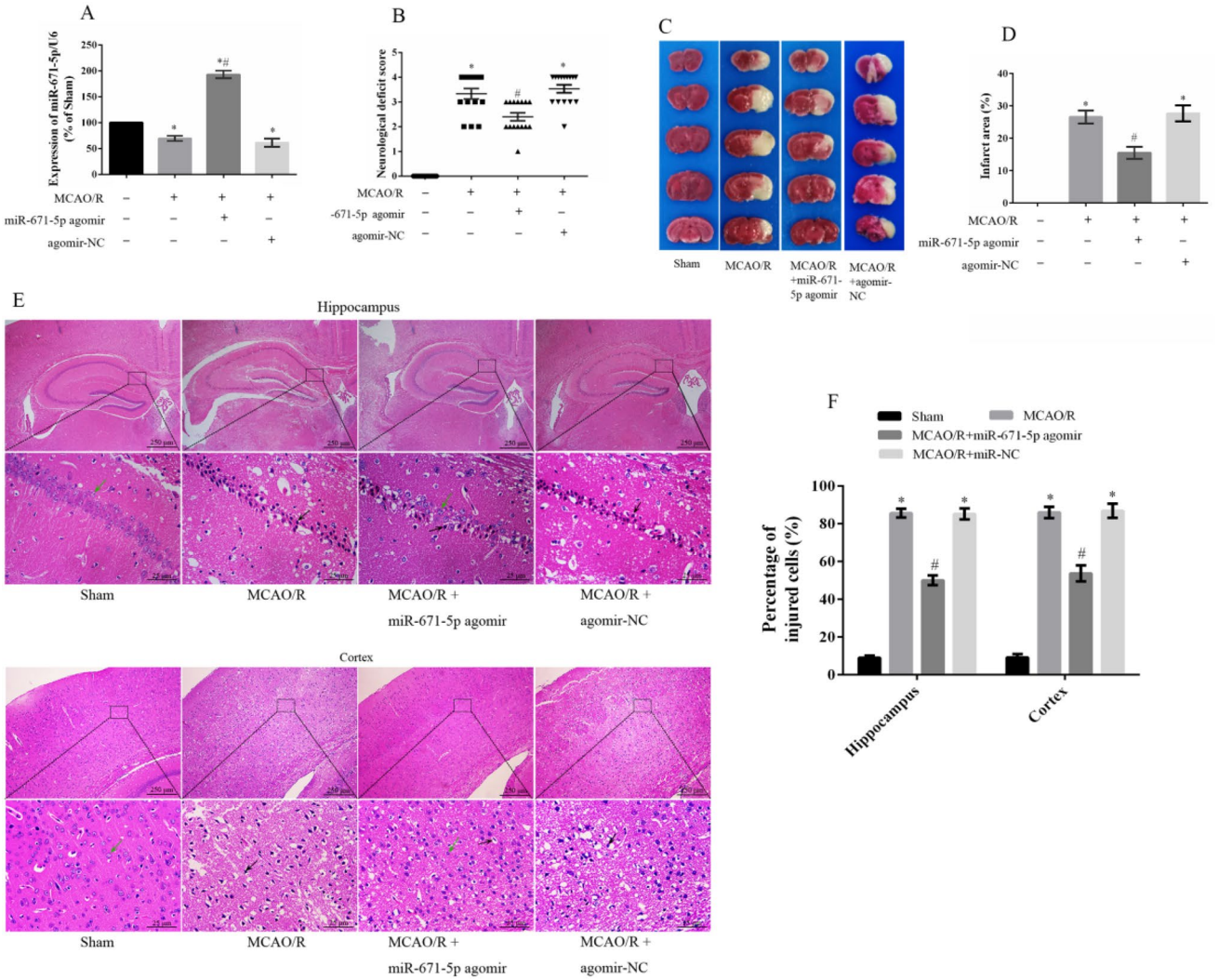

Fig. 4 Impact of miR-671-5P agomir in vivo. **a** Successful upregulation of miR-671-5P expression was achieved, and no significant effects imposed by the negative control were assessed via qRT-PCR ($n = 6$). **b** Neurological deficit scores ($n = 6$). **c**, **d** The area of infarction were measured via TTC ($n = 3$). **e**, **f** H&E staining was used to visualize the injured cells ($n = 3$); green arrow: normal cell, black arrow: injured cell with a reduced nucleus size. One-way ANOVA with Student's *t* test, $^{*}p < 0.05$ vs sham, $^{\#}p < 0.05$ vs MCAO/R group

Neurological deficit scores were increased in the MCAO/R mice group (3.33 ± 0.21, $p < 0.05$) as compared with the sham group (0.00 ± 0.00), but were reduced by in mice treated with the miR-671-5p agomir (2.40 ± 0.16, $p < 0.05$) (Fig. 4b). Our TTC results showed that area of infarction significantly increased after MCAO (26.58% ± 2.00%, $p < 0.05$), but miR-671-5p treatment (15.54% ± 1.86%, $p < 0.05$) significantly decreased the area of infarction (Fig. 4c and d). H&E results showed that cavitation occurred in the tissue and the nucleus of some cells atrophied. Additionally, the number of injured cells significantly increased in the CA1 region of the hippocampus (85.65% ± 2.33%, $p < 0.05$) and cortex (86.03% ± 2.95%, $p < 0.05$) in the MCAO/R group; however, miR-671-5p treatment significantly decreased the injured cells in the hippocampus (50.04 ± 2.61%, $p < 0.05$) and cortex (53.47 ± 4.29%, $p < 0.05$) (Fig. 4e and f). Immunofluorescent NeuN staining showed that the survival of neurons significantly increased in the hippocampal CA1 region and cortex of MCAO/R mice after miR-671-5p agomir treatment (Fig. 5).

miR-671-5p Agomir Reduces MCAO/R-Induced Neuroinflammation via Decreased NF-κB Expression

NF-κB was successfully overexpressed by pcDAN3.1-NF-κB (377.5% ± 42.74%, $p < 0.05$) compared with MCAO/R group (287.60% ± 7.66%), and there was no impact of pcDNA3.1 on the negative controls (287.70% ± 5.69%) in vivo (Fig. 6a). Our qRT-PCR results revealed that *NF-κB* mRNA expression significantly increased after MCAO/R (311.3% ± 12.81%, $p < 0.05$) as compared with the sham group (100.00% ± 0.00%), but the miR-671-5p agomir (184.60% ± 15.18%, $p < 0.05$) significantly decreased levels, which was reversed via NF-κB overexpression (290.50% ± 14.66%) (Fig. 6b). Western blot results revealed that p-P65 and P65 protein levels significantly increased after MCAO/R (p-P65, 0.489 ± 0.015, $p < 0.05$; P65, 0.586 ± 0.037, $p < 0.05$) as compared with the sham group (p-P65, 0.157 ± 0.015; P65, 0.285 ± 0.035), but miR-671-5p treatment significantly decreased levels (p-P65, 0.323 ± 0.032, $p < 0.05$; P65, 0.410 ± 0.020, $p < 0.05$), which was reversed via NF-κB overexpression (p-P65, 0.423 ± 0.018; P65, 0.558 ± 0.037) (Fig. 6c and d). ELISA results showed that proinflammatory cytokines were significantly increased after MCAO (IL-1β, 5.30 ± 0.24 pg/mg, $p < 0.05$; IL-6, 4.70 ± 0.35 pg/mg, $p < 0.05$; TNF-α, 37.22 ± 1.46 pg/mg, $p < 0.05$; iNOS, 41.99 ± 1.19 pg/mg, $p < 0.05$) as compared with the sham group (IL-1β, 2.46 ± 0.25 pg/mg; IL-6, 2.44 ± 0.15 pg/mg; TNF-α, 17.44 ± 1.52 pg/mg; iNOS, 15.28 ± 0.69 pg/mg). miR-671-5p treatment significantly decreased levels of proinflammatory cytokines (IL-1β, 3.61 ± 0.23 pg/mg, $p < 0.05$; IL-6, 3.27 ± 0.16, $p < 0.05$; TNF-α, 26.97 ± 1.88, $p < 0.05$; iNOS, 30.12 ± 2.34, $p < 0.05$), which was reversed after NF-κB overexpression (IL-1β, 4.61 ± 0.17 pg/mg; IL-6, 3.92 ± 0.15 pg/mg; TNF-α, 33.18 ± 1.39 pg/mg; iNOS, 36.57 ± 3.51 pg/mg) (Fig. 6e). Neurological deficit scores were significantly elevated in MCAO/R mice (3.67 ± 0.13, $p < 0.05$), and while these scores were reduced by miR-671-5p treatment (2.13 ± 0.17, $p < 0.05$), NF-κB overexpression reversed these protective effects (3.27 ± 0.18) (Fig. 6f). Fall latency was reduced in the MCAO/R model animals (49.93 s ± 2.63 s, $p < 0.05$) as compared to the sham group (160.00 s ± 0.00 s) in a rotarod test, which was significantly improved by the miR-671-5p agomir (83.27 s ± 3.16 s, $p < 0.05$). However, NF-κB overexpression reversed these effects (57.80 s ± 2.90 s) (Fig. 6g).

Discussion

Our results showed that miR-671-5p expression was reduced in both in vitro and in vivo models of IS. We successfully upregulated or downregulated miR-671-5p by transfecting a siRNA miR-671-5p agomir or antagomir into cells in vitro. Our results showed that upregulated miR-671-5p improved cell viability, reduced cell cytotoxicity, reduced the p-P65 and P65 protein levels, and reduced the levels of proinflammatory cytokines, including IL-1β, IL-6, TNF-α, and iNOS, in OGD/R HT22 cells. Overall, our results showed that upregulated miR-671-5p reduced neurological deficit scores, the area of infraction, p-P65 and P65 protein levels, and the levels of IL-1β, IL-6, TNF-α, and iNOS, and increased the fall latency in MCAO/R mice.

A previous study reported that miR-671-5p participated in the pathogenesis of osteosarcoma [14], breast cancer [16], and osteoarthritis [17]. miR-671 was shown to be highly abundant in the hippocampus of the mammalian brain, and it is bound with the circular RNA Cdr1[19]. miR-671-5p was demonstrated to play an important role in some central nervous system diseases, such as multiple system atrophy and Parkinson's disease [18], and is a target for reducing neuronal toxicity induced by lead poisoning [20]. Our results demonstrated that a miR-671-5p agomir reduced injury and neuroinflammation in both in vitro and in vivo models of IS. These results indicated that miR-671-5p is important for regulating neuronal activity in human and mouse brains.

The overactivation of uncontrolled neuroinflammation exacerbates neuronal death in IS [30]. NF-κB is a transcription factor known to be widely associated with neuroinflammatory responses following ischemic reperfusion [5, 31]. NF-κB is mainly bound to IκB kinase, an NF-κB inhibitor, in the cytoplasm. Shortly after ischemia, the phosphorylation and activation of IκB results in the release of NF-κB from IκB and its subsequent activation, which in turn, induces the upregulation of damaging proinflammatory factors (i.e.,

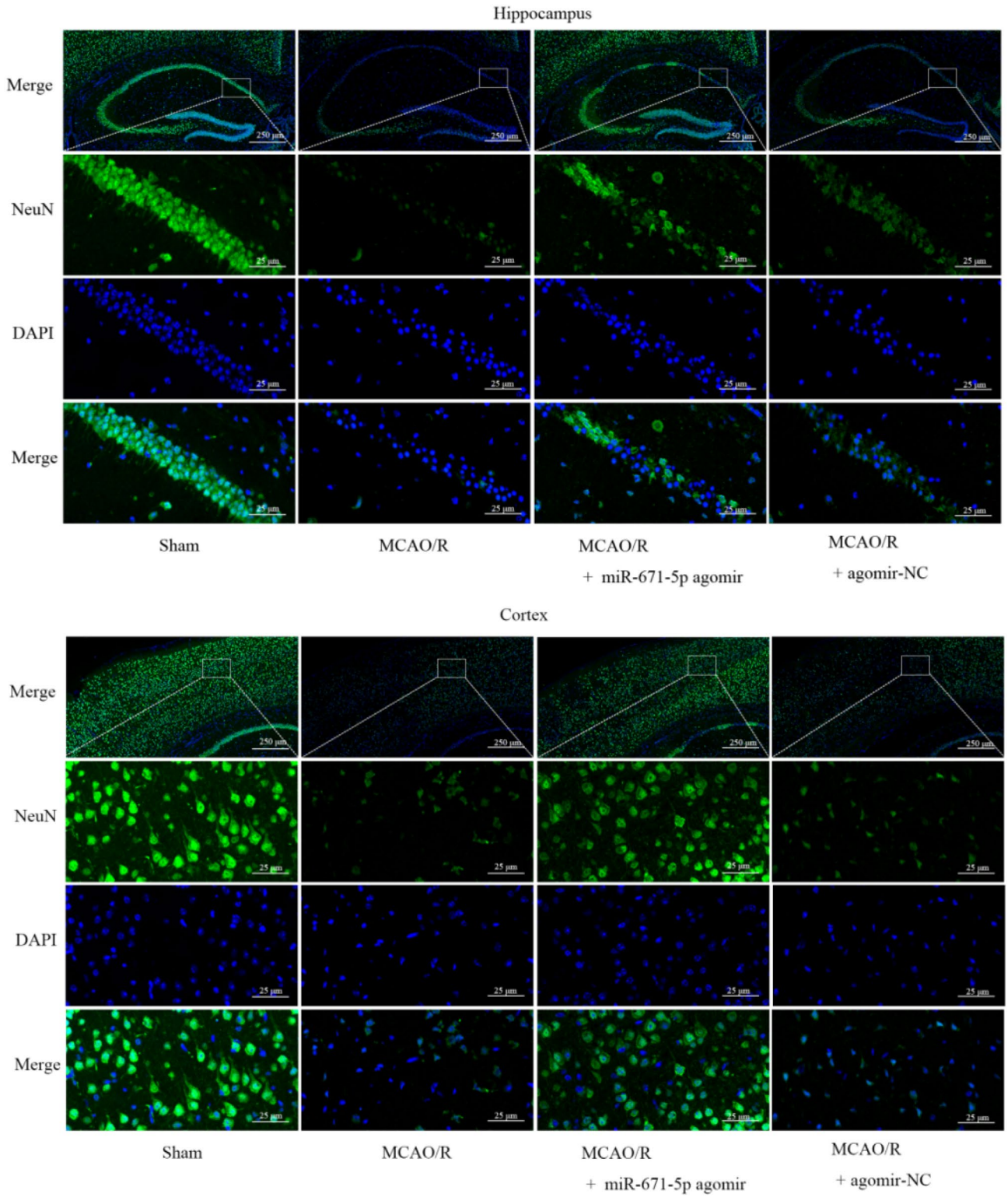

Fig. 5 The effect of miR-671-5p agomir on Neun antibody was analyzed by immunofluorescence in vivo, magnificaion, × 400

IL-1β, IL-6, TNF-α, and iNOS) that aggravate IS-induced neuronal damage [32]. Therefore, suppressing the expression of NF-κB may reduce neuronal death. Our data demonstrated that a miR-671-5p agomir reduced injury and neuroinflammation by suppressing NF-κB expression via a combined treatment of miR-671-5p agomir and pcDNA3.1-NF-κB

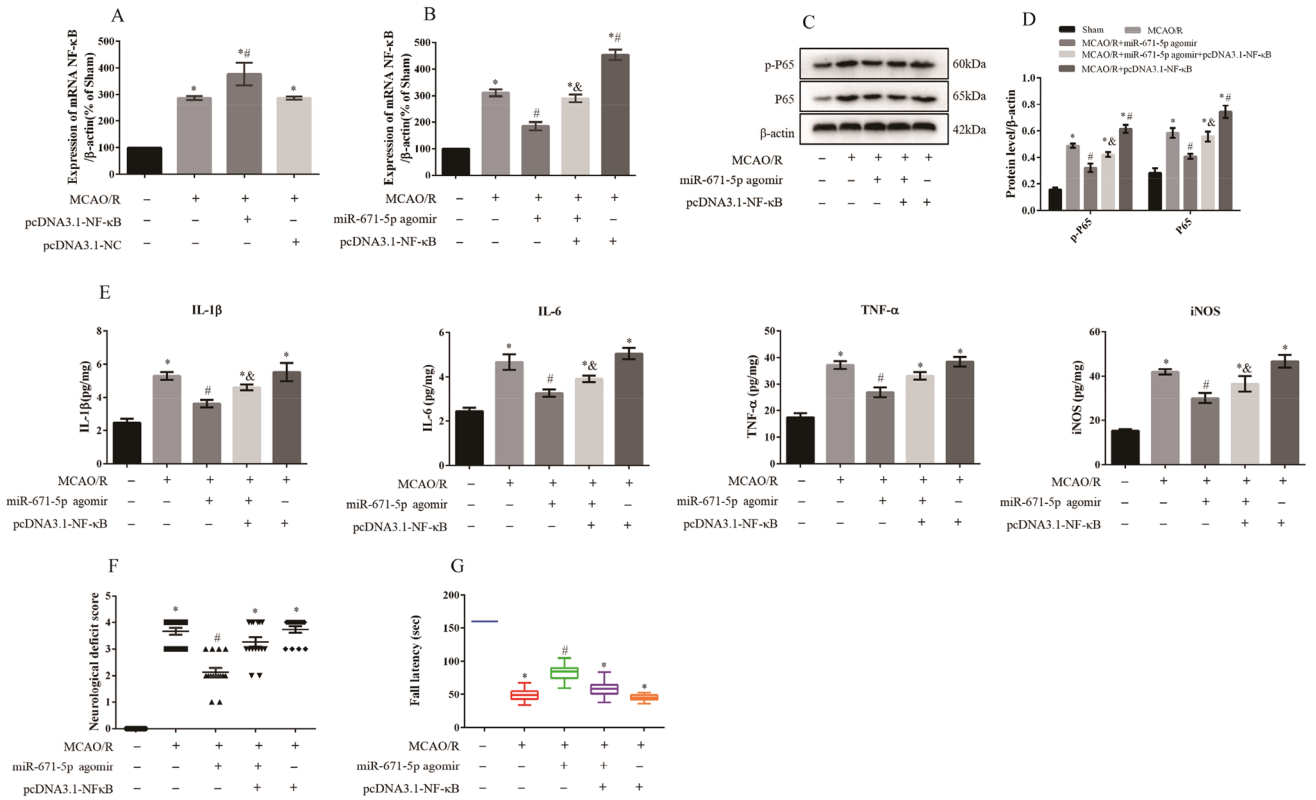

Fig. 6 Impact of miR-671-5P agomir or cotransfection with NF-κB overexpression in vivo. **a** Successful overexpression of mRNA *NF-κB* was achieved, and no significant effects imposed by the negative control were assessed via qRT-PCR ($n=6$). **b** *NF-κB* mRNA expression was assessed via qRT-PCR ($n=6$). **c**, **d** p-P65 and P65 protein levels were assessed via western blotting ($n=6$). **e** IL-1β, IL-6, TNF-α, and iNOS levels were measured via ELISA ($n=6$). **f** Neurological deficit scores ($n=15$). **g** Fall latency seconds of rotarod testing results ($n=15$). One-way ANOVA with Student's *t* test, $^{*}p<0.05$ vs sham, $^{\#}p<0.05$ vs MCAO/R group, $^{\&}p<0.05$ MCAO/R + miR-671-5p + pcDNA3.1-NF-κB vs MCAO/R + pcDNA3.1-NF-κB

both in vitro and in vivo. Our results indicated that miR-671-5p may be a viable therapeutic target for diminishing neuroinflammation in IS patients.

Total NF-κB protein levels have been shown to be elevated in brain tissue samples following cerebral ischemia injury [5, 24], and similar results were detected in this study. This increase in NF-κB protein levels is likely attributed to a combination of hypoxia- and hypoglycemia-induced de novo NF-κB transcription or translation and release of NF-κB resulting from its interactions with IκB. However, since miR-671-5p is an miRNA, it directly interacts with NF-κB at the mRNA level and cannot influence the protein once synthesized. As such, miR-671-5p was unable to alter NF-κB protein activity following its release from IκB. Overall, miR-671-5p reduces neuroinflammation via suppression of NF-κB de novo transcription or translation. Because translation is governed by cytoplasmic ribosomes, total NF-κB levels in the samples were studied without analyzing subcellular localization via western blotting. Cellular immunofluorescence staining indicated that miR-671-5p reduced the cytoplasmic NF-κB levels in HT22 cells after OGD/R. The NF-κB transcription factor can be composed of homodimers or heterodimers of the p50, p52, p65, RelaB, and c-Rel proteins, with p65 being essential for NF-κB functionality [32]. In this study, p65 levels were measured.

Learning and memory problems are a common feature after focal ischemia [33, 34]. The hippocampus serves a critical function in memory, navigation, and cognition. The hippocampus contains the most neurons, and neurons are highly sensitive to irreversible damage caused by ischemia and hypoxia [35]. Following ischemia, constitutively activated NF-κB was found in central nervous system neurons, including the cerebral cortex and hippocampus [36]. Thus, we tried to observe the protective effects of miR-671-5p on the hippocampus in a murine MCAO/R model of IS.

H&E and immunofluorescence staining results showed that miR-671-5p upregulation could reduce nerve cells injured in the cerebral cortex of MCAO/R mice. The cerebral cortex has high levels of astrocytes and microglia, which produce large volumes of proinflammatory cytokines and chemokines following IS [37, 38]. miR-671-5p may play different roles in cortical astrocytes and microglia in the

MCAO/R model, but further studies are needed to support this hypothesis.

Different batches of SYBR green fluorescent dye may have different inherent fluorescence intensity, which may effect the signal of fluorescent intensity and thus the values of gene expression. So percentages of control/sham are used to display the trendency of mRNA NF-κB and miR -671-5p between every group.

Conclusion

Here, we showed that miR-671-5p sufficiently reduced neuroinflammation via suppression of NF-κB expression in both in vitro and in vivo models of IS. The results from our study indicate that miR-671-5p may be a viable therapeutic target for diminishing neuroinflammation in IS patients.

Acknowledgements This study was supported by the Research Innovation of Graduate Students in Chongqing (CYB19165) and General Topics of Basic Research and Frontier Exploration in Chongqing (stc2018jcyjAX0378).We thank LetPub (www.letpub.com) for its linguistic assistance during the preparation of this manuscript. We thank all editors and reviewers for their help and patience.

Declarations

Conflict of interest The authors declare that they have no conflicts of interest.

Ethical Approval Animals were treated in accordance with animal ethics standards throughout the animal experiment.

References

1. Hankey GJ (2017) Stroke. Lancet 389:641–654. https://doi.org/10.1016/S0140-6736(16)30962-X
2. Wu S, Wu B, Liu M, Chen Z, Wang W, Anderson CS, Sandercock P, Wang Y, Huang Y, Cui L, Pu C, Jia J, Zhang T, Liu X, Zhang S, Xie P, Fan D, Ji X, Wong K-SL, Wang L (2019) Stroke in China: advances and challenges in epidemiology, prevention, and management. Lancet Neurol 18:394–405. https://doi.org/10.1016/S1474-4422(18)30500-3
3. Ekker MS, Boot EM, Singhal AB, Tan KS, Debette S, Tuladhar AM, de Leeuw F-E (2018) Epidemiology, aetiology, and management of ischaemic stroke in young adults. Lancet Neurol 17:790–801. https://doi.org/10.1016/S1474-4422(18)30233-3
4. Zhang H, Park JH, Maharjan S, Park JA, Choi K-S, Park H, Jeong Y, Ahn JH, Kim IH, Lee J-C, Cho JH, Lee I-K, Lee CH, Hwang IK, Kim Y-M, Suh Y-G, Won M-H, Kwon Y-G (2017) Sac-1004, a vascular leakage blocker, reduces cerebral ischemia-reperfusion injury by suppressing blood-brain barrier disruption and inflammation. J Neuroinflammation 14:122. https://doi.org/10.1186/s12974-017-0897-3
5. Yang Q, Huang Q, Hu Z, Tang X (2019) Potential neuroprotective treatment of stroke: targeting excitotoxicity, oxidative stress, and inflammation. Front Neurosci 13:1036. https://doi.org/10.3389/fnins.2019.01036
6. Stoll G, Nieswandt B (2019) Thrombo-inflammation in acute ischaemic stroke—implications for treatment. Nat Rev Neurol 15:473–481. https://doi.org/10.1038/s41582-019-0221-1
7. Liu Y, Xue X, Zhang H, Che X, Luo J, Wang P, Xu J, Xing Z, Yuan L, Liu Y, Fu X, Su D, Sun S, Zhang H, Wu C, Yang J (2019) Neuronal-targeted TFEB rescues dysfunction of the autophagy-lysosomal pathway and alleviates ischemic injury in permanent cerebral ischemia. Autophagy 15:493–509. https://doi.org/10.1080/15548627.2018.1531196
8. Kleaveland B, Shi CY, Stefano J, Bartel DP (2018) A network of noncoding regulatory RNAs acts in the mammalian brain. Cell. https://doi.org/10.1016/j.cell.2018.05.022
9. Iyengar BR, Choudhary A, Sarangdhar MA, Venkatesh KV, Gadgil CJ, Pillai B (2014) Non-coding RNA interact to regulate neuronal development and function. Front Cell Neurosci 8:47. https://doi.org/10.3389/fncel.2014.00047
10. Di Y, Lei Y, Yu F, Changfeng F, Song W, Xuming M (2014) MicroRNAs expression and function in cerebral ischemia reperfusion injury. J Mol Neurosci 53:242–250. https://doi.org/10.1007/s12031-014-0293-8
11. Wang S-W, Liu Z, Shi Z-S (2018) Non-coding RNA in acute ischemic stroke: mechanisms, biomarkers and therapeutic targets. Cell Transplant 27:1763–1777. https://doi.org/10.1177/0963689718806818
12. Cheng X, Yang Y-L, Li W-H, Liu M, Wang Y-H, Du G-H (2020) Cerebral ischemia-reperfusion aggravated cerebral infarction injury and possible differential genes identified by RNA-Seq in rats. Brain Res Bull 156:33–42. https://doi.org/10.1016/j.brainresbull.2019.12.014
13. Eyileten C, Wicik Z, De Rosa S, Mirowska-Guzel D, Soplinska A, Indolfi C, Jastrzebska-Kurkowska I, Czlonkowska A, Postula M (2018) MicroRNAs as diagnostic and prognostic biomarkers in ischemic stroke-a comprehensive review and bioinformatic analysis. Cells. https://doi.org/10.3390/cells7120249
14. Xin C, Lu S, Li Y, Zhang Y, Tian J, Zhang S, Yang S, Gao T, Xu J (2019) miR-671–5p inhibits tumor proliferation by blocking cell cycle in osteosarcoma. DNA Cell Biol. https://doi.org/10.1089/dna.2019.4870
15. Lien G-S, Liu J-F, Chien M-H, Hsu W-T, Chang T-H, Ku C-C, Ji AT-Q, Tan P, Hsieh T-L, Lee L-M, Ho JH (2014) The ability to suppress macrophage-mediated inflammation in orbital fat stem cells is controlled by miR-671-5p. Stem Cell Res Ther 5:97. https://doi.org/10.1186/scrt486
16. Tan X, Li Z, Ren S, Rezaei K, Pan Q, Goldstein AT, Macri CJ, Cao D, Brem RF, Fu SW (2019) Dynamically decreased miR-671-5p expression is associated with oncogenic transformation and radiochemoresistance in breast cancer. Breast Cancer Res 21:89. https://doi.org/10.1186/s13058-019-1173-5
17. Zhang B, Sun M, Wang J, Ma C, Hao T, Liu G, Bao G, Zhu Y (2019) MiR-671 ameliorates the progression of osteoarthritis in vitro and in vivo. Pathol Res Pract 215:152423. https://doi.org/10.1016/j.prp.2019.04.015
18. Uwatoko H, Hama Y, Iwata IT, Shirai S, Matsushima M, Yabe I, Utsumi J, Sasaki H (2019) Identification of plasma microRNA expression changes in multiple system atrophy and Parkinson's disease. Mol Brain 12:49. https://doi.org/10.1186/s13041-019-0471-2
19. Piwecka M, Glažar P, Hernandez-Miranda LR, Memczak S, Wolf SA, Rybak-Wolf A, Filipchyk A, Klironomos F, Cerda Jara CA, Fenske P, Trimbuch T, Zywitza V, Plass M, Schreyer L, Ayoub S, Kocks C, Kühn R, Rosenmund C, Birchmeier C, Rajewsky N (2017) Loss of a mammalian circular RNA locus causes miRNA deregulation and affects brain function. Science. https://doi.org/10.1126/science.aam8526
20. Nan A, Chen L, Zhang N, Liu Z, Yang T, Wang Z, Yang C, Jiang Y (2017) A novel regulatory network among LncRpa, CircRar1,

MiR-671 and apoptotic genes promotes lead-induced neuronal cell apoptosis. Arch Toxicol 91:1671–1684. https://doi.org/10.1007/s00204-016-1837-1
21. Luo Y, Ma H, Zhou J-J, Li L, Chen S-R, Zhang J, Chen L, Pan H-L (2018) Focal cerebral ischemia and reperfusion induce brain injury through α2δ-1-bound NMDA receptors. Stroke 49:2464–2472. https://doi.org/10.1161/STROKEAHA.118.022330
22. Orfila JE, Dietz RM, Rodgers KM, Dingman A, Patsos OP, Cruz-Torres I, Grewal H, Strnad F, Schroeder C, Herson PS (2020) Experimental pediatric stroke shows age-specific recovery of cognition and role of hippocampal Nogo-A receptor signaling. J Cereb Blood Flow Metab 40:588–599. https://doi.org/10.1177/0271678X19828581
23. Shi K, Tian DC, Li ZG, Ducruet AF, Lawton MT, Shi FD (2019) Global brain inflammation in stroke. Lancet Neurol 18:1058–1066. https://doi.org/10.1016/s1474-4422(19)30078-x
24. Liu X, Lei Q (2020) TRIM62 knockout protects against cerebral ischemic injury in mice by suppressing NLRP3-regulated neuroinflammation. Biochem Biophys Res Commun 529:140–147. https://doi.org/10.1016/j.bbrc.2020.06.014
25. Zheng L, Huang Y, Wang X, Wang X, Chen W, Cheng W, Pan C (2020) Inhibition of TIM-4 protects against cerebral ischaemia-reperfusion injury. J Cell Mol Med 24:1276–1285. https://doi.org/10.1111/jcmm.14754
26. Pacheco DdF, Pacheco CMdF, Lima MdP, Bader M, Souza AdL, Pesquero JL, Castro Perez A, Duarte IDG (2013) Antinociceptive response in transgenic mice expressing rat tonin. Eur J Pharmacol 713:1–5. https://doi.org/10.1016/j.ejphar.2013.04.032
27. Hayashi K, Hasegawa Y, Takemoto Y, Cao C, Takeya H, Komohara Y, Mukasa A, Kim-Mitsuyama S (2019) Continuous intracerebroventricular injection of *Porphyromonas gingivalis* lipopolysaccharide induces systemic organ dysfunction in a mouse model of Alzheimer's disease. Exp Gerontol 120:1–5. https://doi.org/10.1016/j.exger.2019.02.007
28. Li M, Tian X, An R, Yang M, Zhang Q, Xiang F, Liu H, Wang Y, Xu L, Dong Z (2018) All-Trans Retinoic acid ameliorates the early experimental cerebral ischemia-reperfusion injury in rats by inhibiting the loss of the blood-brain barrier via the JNK/P38MAPK signaling pathway. Neurochem Res 43:1283–1296. https://doi.org/10.1007/s11064-018-2545-4
29. Wang H, Zheng X, Jin J, Zheng L, Guan T, Huo Y, Xie S, Wu Y, Chen W (2020) LncRNA MALAT1 silencing protects against cerebral ischemia-reperfusion injury through miR-145 to regulate AQP4. J Biomed Sci 27:40. https://doi.org/10.1186/s12929-020-00635-0
30. Ji Y, Teng L, Zhang R, Sun J, Guo Y (2017) NRG-1β exerts neuroprotective effects against ischemia reperfusion-induced injury in rats through the JNK signaling pathway. Neuroscience 362:13–24. https://doi.org/10.1016/j.neuroscience.2017.08.032
31. Du X, Xu Y, Chen S, Fang M (2020) Inhibited CSF1R alleviates ischemia injury via inhibition of microglia M1 polarization and NLRP3 pathway. Neural Plast 2020:8825954. https://doi.org/10.1155/2020/8825954
32. Zhan J, Qin W, Zhang Y, Jiang J, Ma H, Li Q, Luo Y (2016) Upregulation of neuronal zinc finger protein A20 expression is required for electroacupuncture to attenuate the cerebral inflammatory injury mediated by the nuclear factor-kB signaling pathway in cerebral ischemia/reperfusion rats. J Neuroinflammation 13:258. https://doi.org/10.1186/s12974-016-0731-3
33. Kathner-Schaffert C, Karapetow L, Günther M, Rudolph M, Dahab M, Baum E, Lehmann T, Witte OW, Redecker C, Schmeer CW, Keiner S (2019) Early stroke induces long-term impairment of adult neurogenesis accompanied by hippocampal-mediated cognitive decline. Cells. https://doi.org/10.3390/cells8121654
34. Kim H, Seo JS, Lee S-Y, Ha K-T, Choi BT, Shin Y-I, Ju Yun Y, Shin HK (2020) AIM2 inflammasome contributes to brain injury and chronic post-stroke cognitive impairment in mice. Brain Behav Immun 87:765–776. https://doi.org/10.1016/j.bbi.2020.03.011
35. Ouyang F, Chen X, Chen Y, Liang J, Chen Y, Lu T, Huang W, Zeng J (2020) Neuronal loss without amyloid-β deposits in the thalamus and hippocampus in the late period after middle cerebral artery occlusion in cynomolgus monkeys. Brain Pathol 30:165–178. https://doi.org/10.1111/bpa.12764
36. Shih R-H, Wang C-Y, Yang C-M (2015) NF-kappaB signaling pathways in neurological inflammation: a mini review. Front Mol Neurosci 8:77. https://doi.org/10.3389/fnmol.2015.00077
37. Jayaraj RL, Azimullah S, Beiram R, Jalal FY, Rosenberg GA (2019) Neuroinflammation: friend and foe for ischemic stroke. J Neuroinflammation 16:142. https://doi.org/10.1186/s12974-019-1516-2
38. Ramírez-Sánchez J, Pires ENS, Meneghetti A, Hansel G, Nuñez-Figueredo Y, Pardo-Andreu GL, Ochoa-Rodríguez E, Verdecia-Reyes Y, Delgado-Hernández R, Salbego C, Souza DO (2019) JM-20 treatment after MCAO reduced astrocyte reactivity and neuronal death on peri-infarct regions of the rat brain. Mol Neurobiol 56:502–512. https://doi.org/10.1007/s12035-018-1087-8

Publisher's Note Springer Nature remains neutral with regard to jurisdictional claims in published maps and institutional affiliations.